

# Compiler Positioning System: An Array Algebra Formulation of Digital Photogrammetry\*

Urho A. Rauhala

General Dynamics/Electronics, P.O. Box 85468, MZ 6108-A, San Diego, CA 92138

**ABSTRACT:** The evolution of array algebra and its applications to the components of the Compiler Positioning System (CPS) will be reviewed, with emphasis on the 1984 to 1988 development period. The CPS removes the restrictions of two-ray stereocompilation by using the array algebra techniques of

- multi-ray Global Least-Squares Correlation (GLSC), which allows transfer of *all* pixels as internal tie points, and
- self-calibrating grid triangulation of dense tie points, automatically forming digital image maps (DIM).

The resulting DIM simplifies and accelerates automatic feature compilation by simple monoscopic pointing. The high accuracy, reliability, and speed of the CPS makes advanced digital photogrammetry practical and economical.

## INTRODUCTION

**P**HOTOGRAMMETRY TODAY is facing fundamental changes due to the advances of digital computer technology. Similar changes started taking place a few decades ago with the birth of analytical techniques in photogrammetric triangulation and stereocompilation. The input of these processes consisted of analog images. Their measured image coordinates were digitized for analytic computations in a computer.

Today, the emphasis of photogrammetric research is shifting toward digital photogrammetry, which has the potential of automating most of the image measurements by utilizing new correlation techniques of digital or digitized *multi-ray* stereo models. The introduction of multiple rays for stereocompilation has the potential of solving the bottlenecks of analog and analytical photogrammetric mapping of two-ray models. However, the rigorous formulation of the combined triangulation and compilation problem of digital photogrammetry has been computationally prohibitive.

Array algebra is a powerful computer and math technology of two decades development that already has solved several computational problems of digital and analytical photogrammetry. Array algebra has grown from the ideas of the photogrammetric and geodetic studies of Rauhala (1968, 1972, 1974) into a broad technology of modern computer and math sciences, (Rauhala, 1975-1987). In summary, array algebra has extended and unified the foundations of

- Vector, matrix, and tensor algebra
- The theory of general matrix inverses
- Estimation theory of mathematical statistics
- Multi-linear numerical analysis
- Digital signal processing and fast transform technology
- Analytical and digital photogrammetry
- Geodetic sciences and potentially all fields involving numerical solutions of large systems of linear and non-linear equations such as meteorology, structural analysis, etc.

The practical computational power of array algebra is based on its general fast transform technique and signal processing which is made applicable for the solution of general systems of linear and non-linear equations by a generalized estimation theory and numerical analysis. This paper will give a brief overview of array algebra and its applications to the components of the compiler positioning system of digital photogrammetry from Rauhala (1986, 1987). The practical proofs of the computational feasibility of on-line DTM validation and progressive sampling

of Rauhala *et al.* (1988) are extended to the array algebra correlation techniques of Global Least Squares Correlation. The philosophy and early applications of array algebra grid triangulations are reiterated.

## FOUNDATIONS AND LITERATURE REVIEW OF ARRAY ALGEBRA

The paper begins with a review of the literature of array algebra and its connection to numerical analysis, mathematical statistics, and fast transform techniques. This is followed by a discussion of some early array algebra applications to problems of medical and industrial close-range photogrammetry.

## MULTI-LINEAR NUMERICAL ANALYSIS

The early development stages of array algebra were reviewed in the Helsinki ISPRS paper of Rauhala (1976). The paper included practical examples of computational solutions from the application of array algebra function theory in a linear regression analysis. The coefficients of a math model for Hardy's multiquadrics, least-squares interpolation, and geodetic boundary value problem were computed at a five-times higher speed than those of equally large two-dimensional Fast Fourier Transforms (FFT). The operations count is linearly dependent only on the number of parameters. The resulting speed of 1,000 nodes in 1.4 CPU seconds can be reached today in general purpose microcomputers and low-end workstations, (Rauhala, *et al.*, 1988).

## LOOP INVERSE ESTIMATION

A common sense interpolation math model for photogrammetric self-calibration and reseau corrections of the Hasselblad close-range moon camera resulted in the foundations of array calculus (Rauhala, 1972). The same technique offered a common sense approach to the problem of a general matrix inverse by a new theory of loop inverses, (Rauhala, 1974, 1975, 1981, 1982).

Loop inverse estimation converts a singular system into the classical full-rank case by replacing the original modeling parameters of an ill-posed problem with an estimable set of functions

$$\mathbf{L}_0 = \mathbf{A}_0 \mathbf{X}, \quad p \leq \text{rank}(\mathbf{A}) \quad (1a)$$

$[\begin{smallmatrix} p,1 \end{smallmatrix}]$      $[\begin{smallmatrix} p,n \end{smallmatrix}]$      $[\begin{smallmatrix} n,1 \end{smallmatrix}]$

from the always estimable space of observables of the Gauss-Markov model

$$\mathbf{E}(\mathbf{L}) = \mathbf{A} \mathbf{X}. \quad (1b)$$

$[\begin{smallmatrix} m,1 \end{smallmatrix}]$      $[\begin{smallmatrix} m,n \end{smallmatrix}]$      $[\begin{smallmatrix} n,1 \end{smallmatrix}]$

\*Presented paper, 16th Congress of the International Society for Photogrammetry and Remote Sensing, Kyoto, Japan, 1-10 July 1988.

The conventional least-squares estimate

$$\hat{L}_0 = \mathbf{H} \mathbf{L} = \mathbf{A}_0 \mathbf{G} \mathbf{L} \quad (2a)$$

provides the estimate

$$\hat{\mathbf{X}} = \mathbf{G} \mathbf{L} = \mathbf{A}_0^m \mathbf{H} \mathbf{L} \quad (2b)$$

by a back substitution of the parameter transformation

$$\hat{\mathbf{X}} = \mathbf{A}_0^m \hat{L}_0, \mathbf{A}_0^m = \mathbf{A}_0^T (\mathbf{A}_0 \mathbf{A}_0^T)^{-1}. \quad (2c)$$

The loop inverse operator  $\mathbf{A}_0^m \mathbf{H}$  turned out to be more general than the pseudo-inverse  $\mathbf{A}^+$ , satisfying all but the condition  $\mathbf{A} \mathbf{G} \mathbf{A} = \mathbf{A}$  of a general inverse. The unique filter operator,

$$\mathbf{H} = (\mathbf{K}^T \mathbf{K})^{-1} \mathbf{K}^T, \mathbf{K} = \mathbf{A} \mathbf{A}_0^m, \quad (3)$$

provided an elegant link between the classical condition and element adjustment techniques (Rauhala, 1974, p. 71). Their expansion to singular systems was straight forward. Yet, the resulting solutions of the singular adjustment problems only involve computations of non-singular square matrices.

Some studies of statistical estimation (Rauhala, 1976) further limited the usefulness of the g-inverse. The fundamental definition of estimability of functions

$$\mathbf{L}_0 = \mathbf{A}_0 \mathbf{X} \text{ by } \mathbf{A}_0 = \mathbf{A}_0 \mathbf{G} \mathbf{A} \quad (4)$$

was extended beyond the restriction of  $\mathbf{A} \mathbf{G} \mathbf{A} = \mathbf{A}$ . These highly theoretical studies resulted in the key philosophy of the Compiler Positioning System for modeling the parameters of Global Least Squares Correlation and automated feature compilation in the always unbiasedly estimable image space of photogrammetry. Summaries of these estimation studies can be found in Rauhala (1981, 1982, 1986, 1987).

#### GENERAL FAST TRANSFORM AND SIGNAL PROCESSING TECHNOLOGY OF ARRAY ALGEBRA

Good (1958) and Cooley and Tukey (1965) applied a special tensor or Kronecker product technique in the derivation of FFT. The transformations of these special tensor products of square matrices were generalized in the array calculus of Rauhala (1972) beyond the Einstein summation convention of tensor calculus. This allowed the expression of overdetermined grid observations as multi-linear functions of separable modeling parameters. Their general solutions by loop inverse estimation (Rauhala, 1972, 1974) provided the tools for covering the unexplored and fertile fields between signal processing, numerical analysis, and mathematical statistics of the adjustment calculus.

The FFT and other fast transforms are very restricted and specialized, yet they are successfully serving several sciences, technologies, and industries. The studies of these special operators helped the array algebra research in finding the philosophy of Array Relaxation (AR) through fast special convolution algorithms. The AR solution of the array algebra finite element and fractal technique of Rauhala (1980a) was applied in the DTM, GLSC, and grid triangulation problems of the compiler positioning system (Rauhala, 1986, 1987) with some further experiments shown in Rauhala *et al.* (1988).

#### ARRAY ALGEBRA USER APPLICATION OF PHOTOGRAMMETRY

Rauhala (1972-1976) reported the early applications of the efficient integration rules of separable math modeling in some odontological and orthopaedic problems of medical photogrammetry. A combined analytical triangulation and multi-ray compilation of a few pre-targeted discrete object points provided their accurate object space coordinates. The array algebra regression technique was used for an efficient least-

squares fitting of a mathematical model into the measured coordinates. The resulting model was used to derive volumetric, relative bone movement, and other data of user interest, as shown in Lippert (1973), Bergstrom (1974), and Rauhala (1976).

The development of the STARS close-range system of industrial photogrammetry and the use of its predecessor for accurate volumetric and other calibrations of LNG transport and storage tanks occupied most of the 1975 to 1983 professional implementations of array algebra (Brown, 1984; Rauhala, 1976-1987). This photogrammetric tank calibration procedure became the accepted standard of the industry after the National Bureau of Standards had certified the technique through independent tests. (Siegarth *et al.*, 1984).

The analytical system of STARS is a specialized form of the digital CPS concept as discussed by Rauhala (1987). The new automated image mensuration system of Global Least Squares Correlation in future digital or digitized systems of industrial photogrammetry could eliminate the need for manual preselection and retargeting of the object points to be measured. An on-line AR feedback loop of the finite element progressive surface modeling could automatically determine the optimal number and location of the points to be measured until a prespecified modeling accuracy of the quantities of user interest is achieved.

Examples of the on-line AR modeling algorithms are the experimental three-dimensional (time dependent) STARS reseau reduction technique of array algebra and the automated DTM validation technique. The technique of entity LSC of the object surface will reduce or eliminate the need for discrete point targeting in several applications. Examples include the calibration of the actual object shape against its design shape, and the removal of the cumbersome monumentation and pretargeting requirements in the CPS and hypertriangulation technology of national and continental surveys down to the scale of cadastral surveying (Rauhala, 1968, 1986, 1987). The beauty of GLSC and the array algebra reseau correction technique is that one high quality reseau or retro-target measurement of a discrete point can be replaced by several lower quality and very fast sub point measurements of GLSC. The final product quality is controlled on-line such that the overall production of the user application is accelerated by orders of magnitude. For more literature, see Masry (1981), Lugnani and Souza (1984), and Rosenholm and Torlegard (1987).

#### COMPILER POSITIONING SYSTEM (CPS)

The concept of the CPS in digital photogrammetry integrates an automated multi-ray stereo mensuration of image-to-image pixel transfer functions with a rigorous self-calibrating array algebra grid triangulation of their accurate object space coordinates. The main philosophical and practical problems of this new digital formulation of photogrammetry are discussed by Rauhala (1986, 1987) with some practical examples of its key algorithms summarized in Rauhala *et al.* (1988). In a very brief summary, these main problems are

- *Data acquisition, storage, transfers, reformatting, and processing of digital stereo images.* Image processing techniques typically have handled only small non-metric images so that even a brute-force conversion of two-ray analytical stereo compilation into the digital domain appears cumbersome. The two-ray digital stereo compiler would still share the main shortcomings of the old analog and analytical photogrammetry, leaving the main potential advantages of digital photogrammetry unexplored.
- *New systems components.* The systems and operations concepts tailored for two-ray compilation in analog and analytical photogrammetry have to be replaced by new ones before full advantage can be taken of digital photogrammetry. The computational problems of the new system components of multi-stereo CPS have prompted several inventions and practical developments of the array algebra

technology that make the introduction of CPS practically feasible in the foreseeable future.

The next sections will reiterate the philosophy of the three main system components, namely:

- automated mensuration of the pixel mapping functions of Global Least Squares Correlation (GLSC),
- grid triangulation, and
- automated information extraction from a Digital Image Map (DIM).

Following that, some experimental work in the implementation of these new techniques and concepts will be summarized.

#### PIXEL TRANSFER TECHNIQUE OF GLSC

The GLSC process replaces the selective, usually manual, single-point image coordinate measurements of a few discrete multi-ray tie and two-ray compilation points of analytical photogrammetry by a rigorous simultaneous multi-ray image-to-image transfer solution of *all* pixels. This involves rigorous least-squares solutions of the finite element modeling parameters of the shifts and radiometric biases. The minimum number of modeling parameters depends on the behavior of these shift and bias functions. Therefore, the feedback loop of progressive sampling and on-line validation of the modeling quality is integrated into GLSC.

For many practical applications, we are interested not only in the minimum number of the parameters for a sufficient modeling accuracy but also in their evaluations of the shift parameters at a dense regular grid. This grid simplifies the evaluation of the shifts at the pixel level by a simple local interpolation. Thus, once this grid of the finite element technique is established, we have implicitly transferred the geometric location (and radiometric distortion) of every single pixel of the reference image to the slave images. This opens the new fields of "stereo" image enhancement and "multi-ray stereo" image coding.

In order to automate the compilation (feature extraction) problem with a sufficient accuracy and image resolution of DIM, the grid has to be quite dense. Ideally, we would like to capture the image space shift behavior of the object's micro-surfaces such as the resolvable terrain canopy. This typically requires the use of such high node density and small correlation windows that single-point correlation techniques would break down in reliability and production speed. The philosophy of the simultaneous global solution prevents this breakdown as will be shown in some examples of practical tests in the section on Experimental Results.

One would think that the computational solution of the global formulation is unfeasible as its special case of solving the unconstrained diagonal system of the single-point approach of the conventional formulation would be too slow. However, here the power of the GLSC philosophy and array algebra computer technology can be utilized such as that envisioned by Rauhala (1977-1987) in the global solution and concurrent sample speeds of over millions of parameters per second. The feasibility of these future advanced systems of tailored hardware is shown by the slower software experiments in the section on Global Least Squares Correlation.

#### GRID TRIANGULATION

The dense point transfer grid of GLSC in image space provides the input of grid triangulation. The self-calibration math model is extended to image variant self-calibration to allow for shear free and high density object space coordinates to the dense image transfer grid. Each enhanced (magnified image) has local image-to-object and object-to-image grid transforms so they can be considered as Digital Image Maps (DIM) (Rauhala, 1986-1987).

#### USE OF DIGITAL IMAGE MAP

DIM makes the use of orthophotos and compilation of line maps obsolete from the point of view of the map user. A monoscopic DIM pointing yields the object surface coordinates in real-time. Rauhala (1986-87) discusses the future possibility of digital multi-ray stereo instrument for a "hologrammetric" type of mensuration of multi-layer features and the final edit of the "geometrically" enhanced or magnified DIM.

#### EXPERIMENTAL RESULTS

*Grid Triangulation.* Rauhala (1972, 1974, 1975) reported some 1970-71 grid triangulation results for a 5 by 9 strip test field constructed on a wall of a camera calibration laboratory in Stockholm. Both image variant and invariant "discrete" self-calibration parameters were applied with and without simultaneous geodetic observations. Full variance-covariances among all control points could be incorporated because the reduced normals were expressed in terms of the coordinate and image invariant self-calibration parameters. These experiments introduced multiple exposures and discrete image and point variant reseau corrections for self-calibration of the only discretely unbiasedly estimable systematic errors of the "tie grid." This concept grew into "hyper-triangulation" and "hyper-compilation" of digital systems of enormous accuracy potential. The fundamental realization that the unbiased self-calibration is possible only at the discrete image grid locations of the regular tie grid is not yet commonly understood in photogrammetry. It explains a critical flaw of the control transfer in analytical photogrammetry for arbitrarily distributed control points (Rauhala, 1980d, 1986, 1987). This and several other critical flaws of analytical triangulation are removed by the concept of hyper-triangulation.

A new solution of the photogrammetric bundle adjustment was experimented in the early 1970s using the loop inverse modifications of orthogonalization and hyper Cholesky techniques (LSQCHOL) of singular and non-singular matrices (Rauhala, 1975, 1987). This algorithm is computationally superior to the traditional elimination, banded-border solution, and error propagation techniques of analytical photogrammetry as discussed in more detail by Rauhala (1987). The achieved accuracy of 0.1 to 0.2 micrometres in the image scale of the 1970-71 "tie grid" triangulation is not yet common in photogrammetric literature. The feasibility of the expansion of the sparse 5 by 5 "image tie grid" triangulation of the early experiments to the dense GLSC image transfer grid was established computationally by Rauhala (1982, 1984). The applications of the self-calibrating net adjustments of the North American Datum and inertial survey traverses employ the same computational mechanism as the GLSC tie grid triangulation with image variant self-calibration of the finite element techniques of array algebra, as shown by Rauhala (1986, 1987).

*On-Line DTM Validation.* The on-line DTM validation algorithm grew from the experimental development of array algebra and loop inverse filtering. Rauhala (1972-1978) and Rauhala and Gerig (1976) report several simulations of the loop inverse interpolators:

$$\mathbf{K} = \mathbf{A}\mathbf{A}_0^{-1} \text{ and filters } \mathbf{H} = (\mathbf{K}^T\mathbf{K})^{-1}\mathbf{K}^T \quad (5)$$

for extremely efficient data snooping and the least-squares solution technique of array algebra signal processing. Some of these new techniques were implemented in the DTM validation experiments of Rauhala (1980a, 1980c, 1980d).

The AR solution technique of the 1980 finite element DTM study opened the practical GLSC solution of the linearized array correlation formulation of Rauhala (1977). The global solution part of the GLSC algorithm was tested during 1980-82 on an experimental three- and four-dimensional finite element reseau

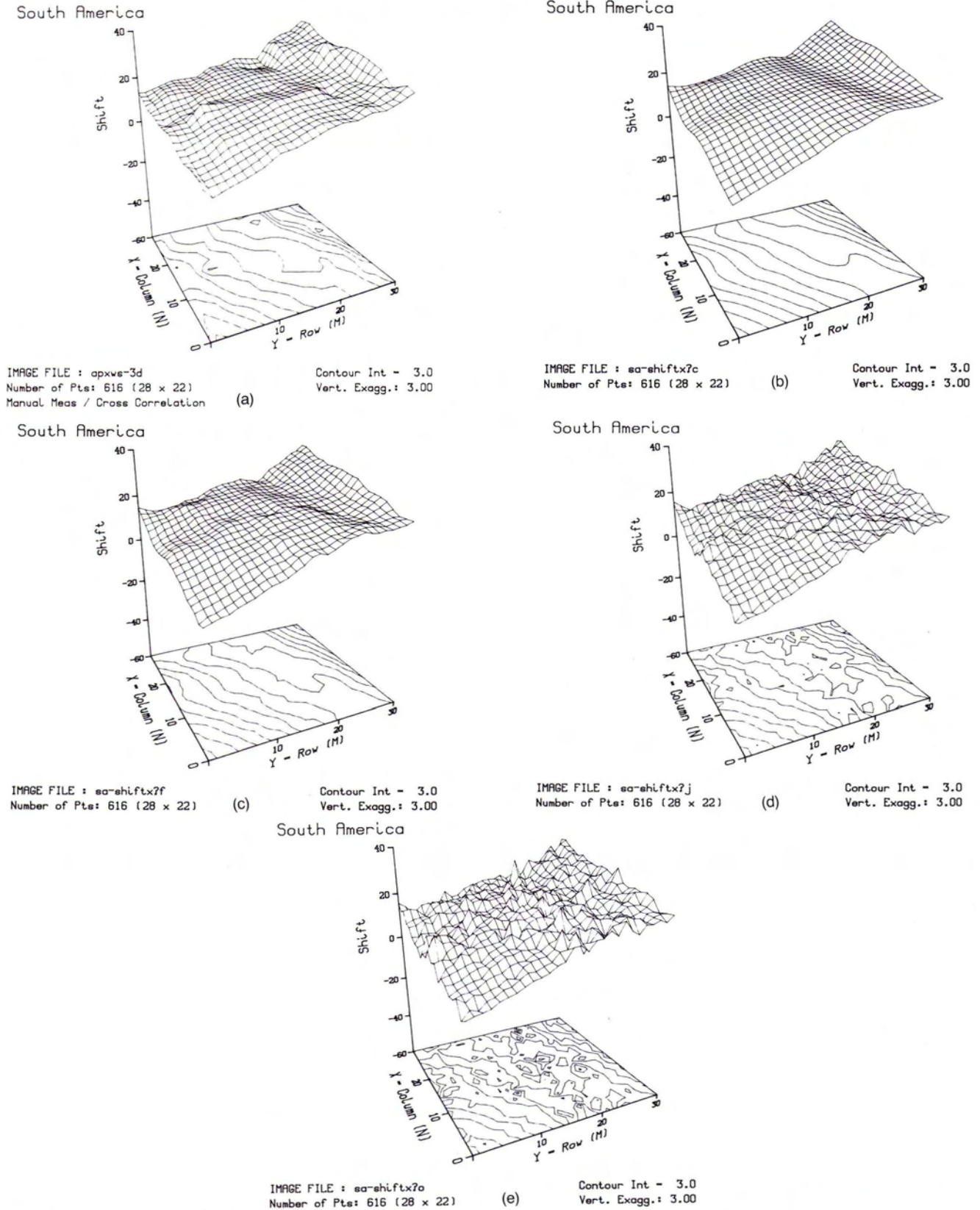


FIG. 1. (a) Initial  $8 \times 8$  pe x-shift grid of South America (SA) data, 1 pe = 0.5 m. (b) GLSC x-shift solution of SA data with a tight continuity weight. (c) GLSC x-shift solution of SA with an optimal continuity weight. (d) GLSC x-shift solution of SA data with a relaxed continuity weight. (e) GLSC x-shift solution of SA data with zero continuity weight.

Car - Sig Slope Pull-in Shifts

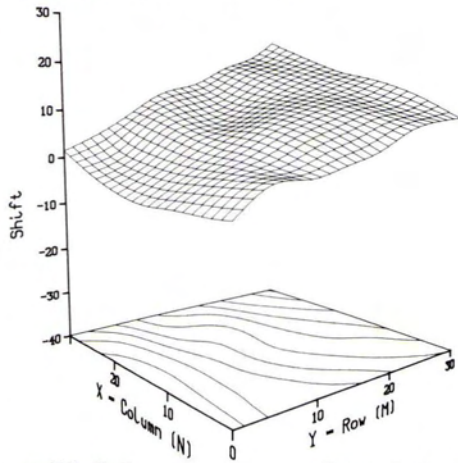


IMAGE FILE : ceehiflx7init  
Number of Pts: 616 (28 x 22)  
Significant Slope Shifts

(a)

Contour Int - 3.0  
Vert. Exagg.: 3.00  
Ref Var - 12.340 gray shades

Car - Shifts

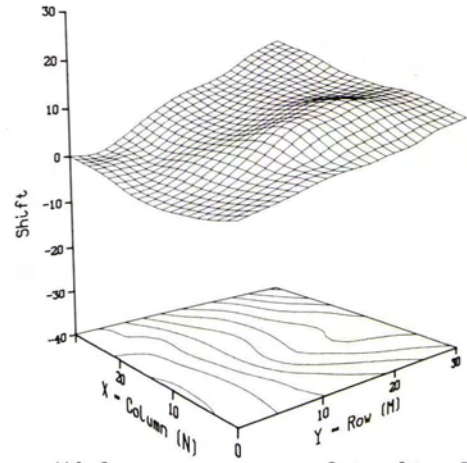


IMAGE FILE : ceehiflx7c  
Number of Pts: 616 (28 x 22)  
Significant Slope

(b)

Contour Int - 3.0  
Vert. Exagg.: 3.00  
Ref Var - 5.474 gray shades

Car - Shifts

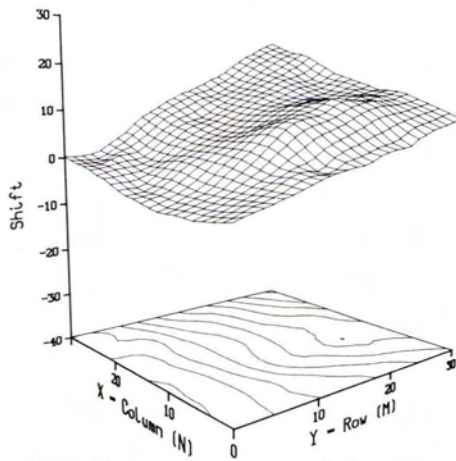


IMAGE FILE : cldshiflx7h  
Number of Pts: 616 (28 x 22)  
1-D GLSC Seeds

(c)

Contour Int - 3.0  
Vert. Exagg.: 3.00  
Ref Var - 5.422 gray shades

Car - Converged Solution after 15 iterations

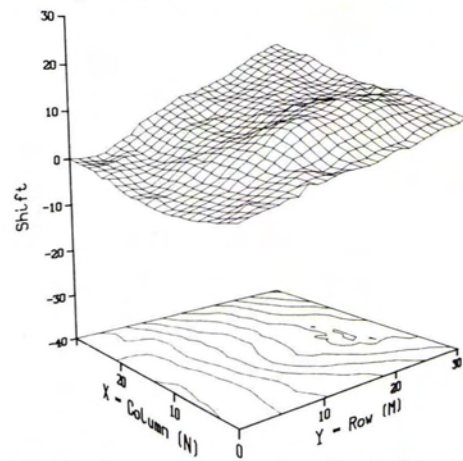


IMAGE FILE : carehiflx7o  
Number of Pts: 616 (28 x 22)  
5 x 5 sampling window

(d)

Contour Int - 3.0  
Vert. Exagg.: 3.00  
Ref Var - 5.3 gray shades

FIG. 2. (a) Fast  $8 \times 8$  pe x-shift pull in grid of Car 1 (Car) data, 1 pe = 0.4 mm. (b) GLSC x-shift solution of Car data with a tight continuity weight. (c) GLSC x-shift solution of Car data with an optimal continuity weight. (d) GLSC x-shift solution of Car data with zero continuity weight.

correction technique of CRC-1 camera of STARS. It was also applied in the grid triangulation simulations of Rauhala (1982, 1984).

The solution of GLSC is very closely related to the finite element DTM AR of progressive sampling. Therefore, the 1984-88 research effort of the integrated CPS concept started from a refined experimental implementation of the on-line DTM validation and progressive sampling of the AR algorithm. The technique and the results of the extensive experiments are reported in Rauhala (1986, 1987) and Rauhala *et al.* (1988). The automated on-line integration of the product validation into the measurement process significantly improved the quality, speed, and economy of DTM generation as expected. An experiment provided an output rate of 533 nodes/sec of the automatically validated DTM with a reliability exceeding that of an experienced operator.

**Global Least-Squares Correlation.** The report (Rauhala *et al.*, 1988) summarizing the on-line DTM validation experiments contains over 50 pages, so the more extensive experiments of GLSC have to be greatly condensed as follows:

**Micro-topography Correlation:** The critical flaws of all single-point correlation techniques (including multi-ray LSC) is removed

by GLSC, allowing high quality correlation of an object's micro-topography. The result is illustrated in Figure 1 at the  $8 \times 8$  pe node density of "South America" (SA) ISPRS test data of epipolar geometry. The process of GLSC was initiated from the best available pull-in parallax values of Figure 1a provided by the manually edited/filled-in values of conventional cross-correlation at  $16 \times 16$  pe intervals and interpolated to the  $8 \times 8$  pe density. The finite element model of the x-shifts had overly tight continuity constraints in the first iteration (Figure 1b). The constraints were loosened in each iteration to illustrate the capability of GLSC to capture the detailed micro-topography (Figures 1c and 1d) with the optimal and relaxed continuity weights.

Figure 1e illustrates the inherent weakness of the single-point correlation techniques corresponding to zero continuity weight of the global parallax model. Although the previous iterations yielded the ultimate pull-in and reshaping values, the solution diverges at several "adverse" areas that, through the incorrect reshaping values, start polluting the neighboring "good" points. We may have found an explanation for the frequent failures of the conventional single-point correlation as illustrated in Figure

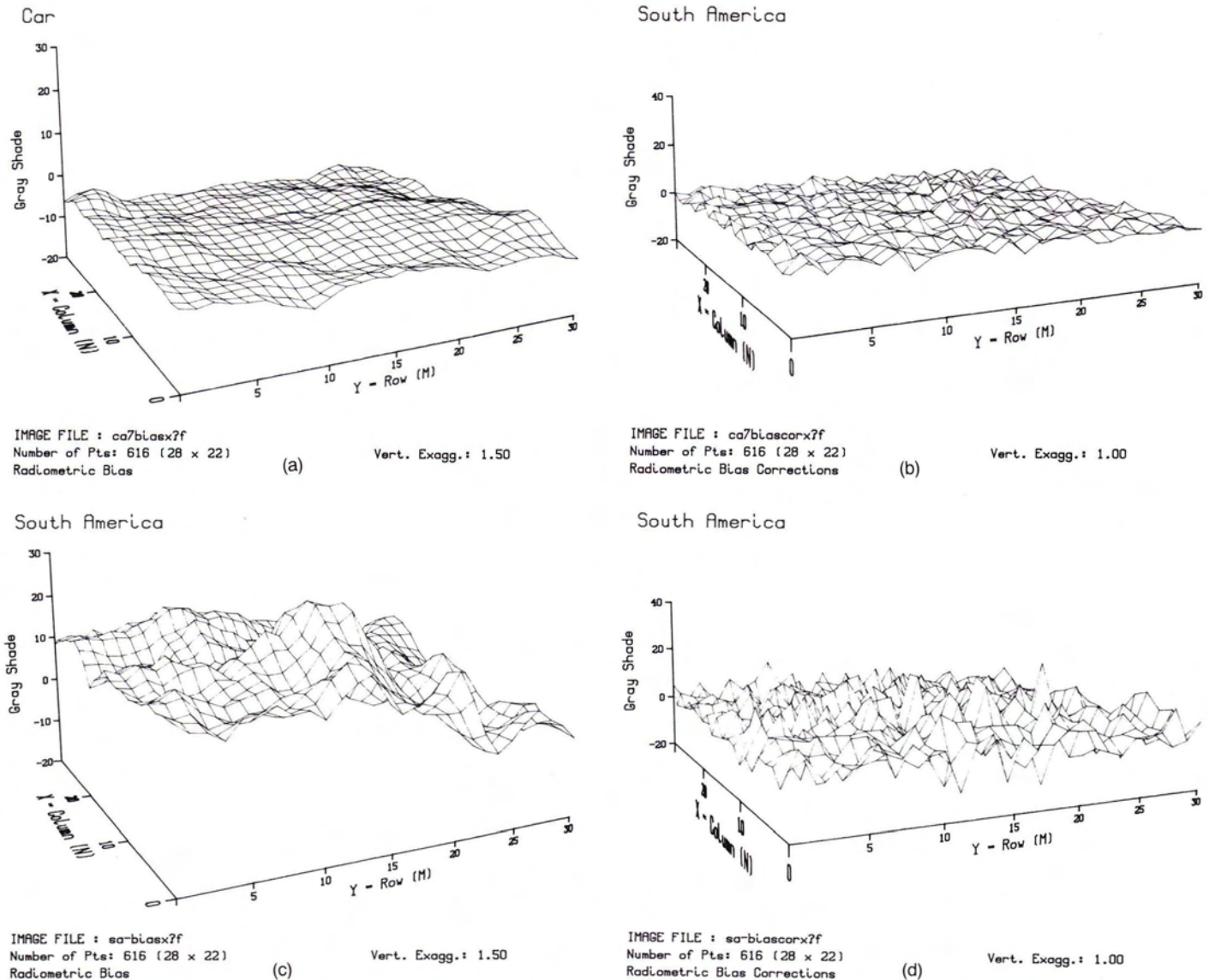


FIG. 3. (a)  $3 \times 3$  shaping average of radiometric bias of optimal Car solution. (b) Correction terms of radiometric bias of optimal Car solution. (c)  $3 \times 3$  shaping average of radiometric bias of optimal SA solution. (d) Correction terms of radiometric bias of optimal SA solution.

3. Figure 2 shows another epipolar example where the single-point technique converges with the help of the refined GLSC pull-in process.

*Rigorous Modeling of Radiometric Bias in GLSC:* The above GLSC experiment with  $7 \times 7$  sample windows at all nodes of  $8 \times 8$  pe spacing (no progressive sampling) was repeated with  $7 \times 7$ ,  $5 \times 5$ , and  $3 \times 3$  sample windows of the "Car I" stereo model. The automated cross-correlation succeeded at all attempted pull-in points. The differences RMS of the GLSC and the cross-correlation results was smallest (0.4 pe) in the over-smoothed case of GLSC of Figure 2b. As the continuity weight is released, the actual shape of  $x$ -shifts resolvable by the  $8 \times 8$  pe node spacing becomes evident as shown in Figure 2c. The RMS difference to cross-correlation is only slightly increased, but local deviations up to 1.1 pe are found. This time, the GLSC iterations with decreased continuity weights stabilized to the unique point-wise LSC solution of Figure 2d, even with the small windows. The iteration process of GLSC gradually refines the reshaping and local pull-in values until the fine LSC samples become possible.

The initial values of Figure 2a GLSC test were found by an

efficient one-dimensional GLSC process and two-dimensional interpolation scheme of array algebra, yielding accuracies on the order of a few pixels (Rauhala, 1986, 1987). The solution converged exactly to the same unconstrained point-wise LSC  $x$ -shifts as before with the initial pull-in values from cross-correlation. The results of these tests with Car I data confirm those of SA data that the conventional point-wise (or, rather, area) cross-correlation is capturing only the smoothed (tight continuity weight) or averaged shift values, perhaps because of the habitual use of too large windows to avoid the breakdown. But why such large windows to avoid the breakdown? The rigorous modeling of the radiometric biases of GLSC can perhaps explain the fact that Car I image data allowed the unconstrained LSC solution while the SA GLSC solution diverges at several "adverse points" if the neighborhood constraints are released too much.

Figure 3 shows the radiometric bias terms of the shaping and correction processes of Car I and SA data. The shaping terms are  $3 \times 3$  averages of the accumulated bias corrections used for reshaping in each iteration. The correction terms are a part of

Island

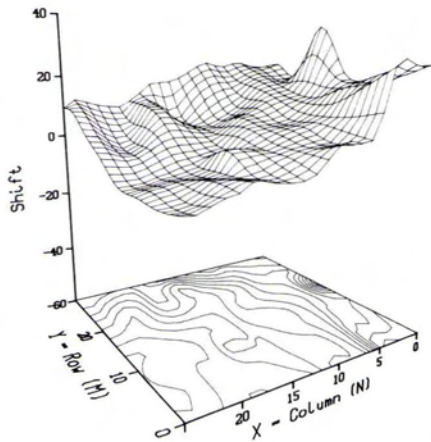


IMAGE FILE : l1dshiftx7init  
Number of Pts: 616 (28 x 22)  
1-D GLSC seeds

(a)

Contour Int - 3.0  
Vert. Exagg.: 3.00  
Ref Var - 19.196 gray shades

Island

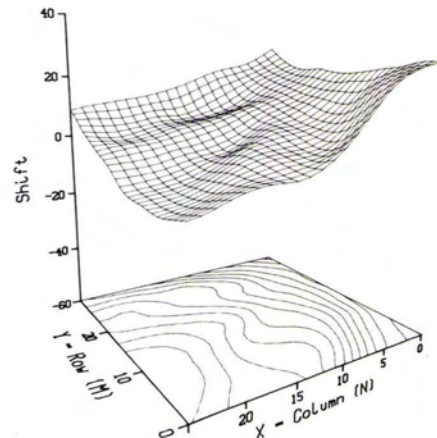


IMAGE FILE : l1dshiftx7c  
Number of Pts: 616 (28 x 22)  
1-D GLSC seeds

(b)

Contour Int - 3.0  
Vert. Exagg.: 3.00  
Ref Var - 12.205 gray shades

Island

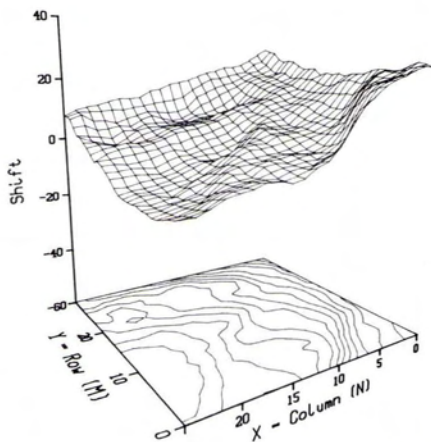


IMAGE FILE : l1dshiftx7h  
Number of Pts: 616 (28 x 22)  
1-D GLSC seeds

(c)

Contour Int - 3.0  
Vert. Exagg.: 3.00  
Ref Var - 11.496 gray shades

Island

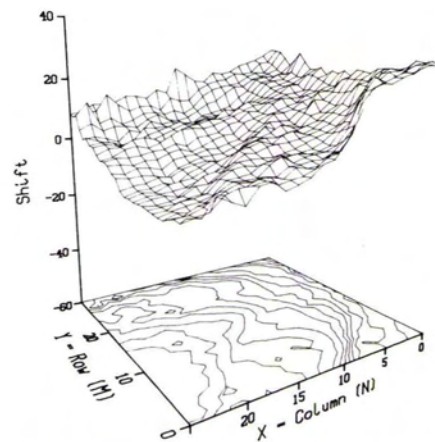


IMAGE FILE : l1dshiftx7o  
Number of Pts: 616 (28 x 22)  
1-D GLSC seeds

(d)

Contour Int - 3.0  
Vert. Exagg.: 3.00  
Ref Var - 10.3 gray shades

FIG. 4. (a) Fast 8 x 8 pe x-shift pull-in grid of Island (Is) data, 1 pe = 0.1 m. (b) GLSC x-shift solution of Is data with a tight continuity weight. (c) GLSC x-shift solution of Is data with an optimal continuity weight. (d) GLSC x-shift solution is data with zero continuity weight.

LSC sample solutions where their magnitude is properly constrained without the rigorous global continuity constraint. The bias shaping and correction terms of Car I data are very smooth and small in comparison to the SA data. These terms reflect the image quality and correlatability of stereo images together with the standard error of unit weight,  $s_o$ , and standard errors for the LSC samples. Car I had an  $s_o = 4$  to 5 gray values and SA data had a low  $s_o$  only at the "good" points. The standard error of x-shifts varied in the range of 0.05 to 0.2 pe.

The main reason for the breakdown of point-wise LSC with SA data is the fact that the effect of radiometric bias cannot be separated from the effect of the shift on a point-wise basis at small windows. SA data have poor contrast such that the reduced normal equation for the shift parameter after the elimination of the bias correction becomes ill-conditioned for small windows even if the bias correction is allowed to move only within the noise level. The global continuity constraints of GLSC for the x-shifts and the refined reshaping/pull-in process have the strength of overcoming this and other shortcomings of single-point correlation.

*Large Pull-in Range of GLSC:* The concept of the global linearized math model (parallax DTM) of array algebra function theory in Rauhala (1977) was prompted by the intuitive idea of computing refined pull-in values to "bridge small sub-spaces" of hidden surfaces or adverse areas. The gradual pull-in of the iterative linearized GLSC process of non-linear correlation was, also intuitively, conceived as the mechanism for increasing the overall pull-in range of a complete frame (1K x 1K pe). This is far beyond the restricted local pull-in range of LSC samples. This may explain why the LSC technique alone could not immediately capture the enthusiasm of correlation experts (Helava, 1987). This limited pull-in of LSC also explains the rather discouraging reliability and overly optimistic error propagation of the well known tests of the Stuttgart and Stockholm Photogrammetric Institutes.

Both of the above intuitive ideas turned out to be right. Our experiments have demonstrated the capability of GLSC to bridge over a sharp blunder or a break-line using the poor SA data. A gradual automated fill-in of GLSC covered an "adverse area" of a sub grid over 20 pe blunders. Similar tests were made for the

Wall

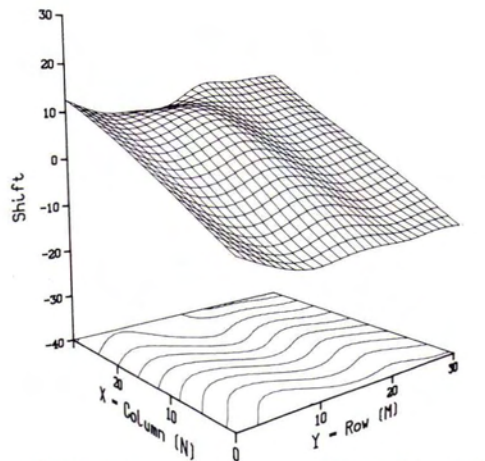


IMAGE FILE : wa7ehiftx7init  
Number of Pts: 616 (28 x 22)  
Pull-in Shifts

(a)

Contour Int = 3.0  
Vert. Exagg.: 3.00

Wall

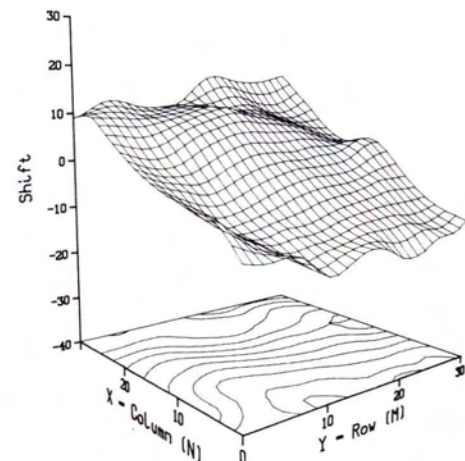


IMAGE FILE : wa7ehiftx7c  
Number of Pts: 616 (28 x 22)

(b)

Contour Int = 3.0  
Vert. Exagg.: 3.00

Wall

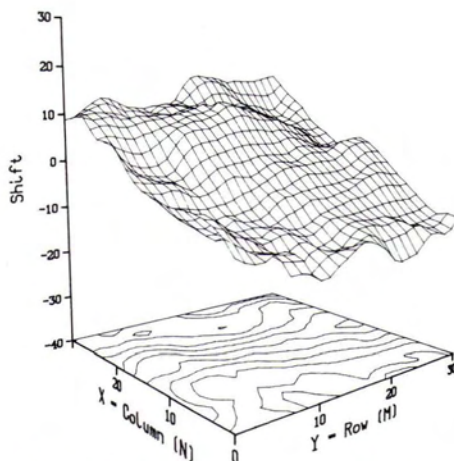


IMAGE FILE : wa7ehiftx7f  
Number of Pts: 616 (28 x 22)

(c)

Contour Int = 3.0  
Vert. Exagg.: 3.00

Wall

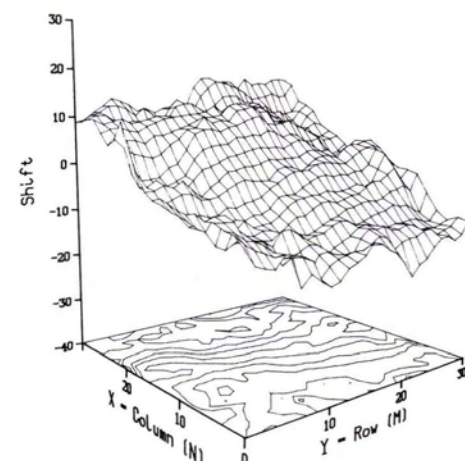


IMAGE FILE : wa7ehiftx7j  
Number of Pts: 616 (28 x 22)

(d)

Contour Int = 3.0  
Vert. Exagg.: 3.00

FIG. 4. (e) Fast  $8 \times 8$  pe x-shift pull-in grid of Wall data, 1 pe = 2 mm. (f) GLSC x-shift solution of Wall data with a tight continuity weight. (g) GLSC x-shift solution of Wall data with an optimal continuity weight. (h) GLSC x-shift solution of Wall data with a relaxed continuity weight.

overall pull-in range of SA data by the introduction of over 20 pe blunders in some initial values that by the pull-in process contaminated a large region of the frame. The correct robust solution of micro-topography was recaptured although the number of iterations was increased. However, the GLSC formulation of array algebra has some superior computational qualities, allowing a large number of iterations as discussed next. Figure 4 is shown as an example of the pull-in range of the fully automated GLSC with respect to "Island" and "Wall" epipolar imagery of the ISPRS test data. Figure 5 shows the radiometric bias solutions of these data sets. The results of Figures 1 to 5 reflect the use of  $7 \times 7$  pe correlation windows with 100 percent sampling of nodes at the  $8 \times 8$  pe interval.

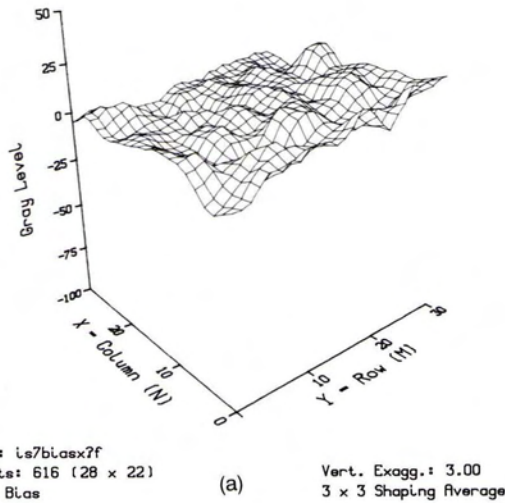
*Speed and High Quality of GLSC Is Economy:* The LSC sample process of GLSC requires

- Reshaping of only a few pixels of a small window of a slave image versus large windows of both images for traditional cross-correlation;
- Product sums of a small window versus large windows; and
- No repetition of the above processes for 8 to 16 trial centers of the non-linear cross-correlation. This means that the refined sample

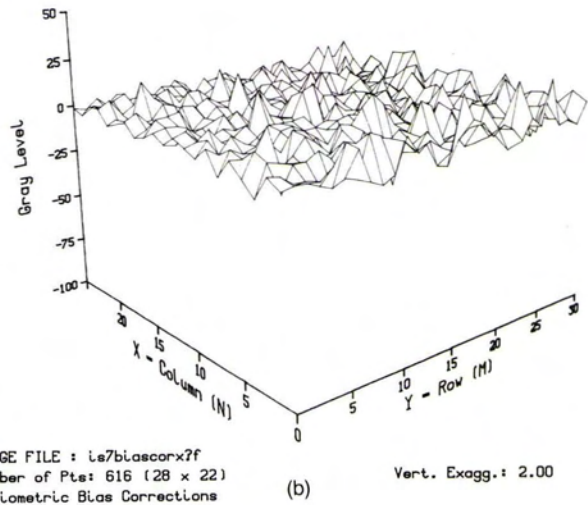
process and the linearized global solution can be iterated several times in the fashion of automated progressive sampling of Rauhala *et al.* (1988) to avoid over- or under-sampling. The iteration process can be accelerated by some common sense strategies or by the exciting new technique of non-linear least squares of Blaha (1987).

The sample process of one GLSC iteration requires an order of magnitude less arithmetic operations than any other known technique. The "impossible dream" of a general purpose microprocessor implementation is thereby realized for the digital photogrammetric correlation problem. We have experienced in the order of 100 to 1,000 times higher software solution speeds in comparable computers than most of the other emerging LSC and related object reconstruction techniques found in the literature; for examples, Rosenholm (1986), Gruen and Baltasvias (1986, 1987), Helava (1987), Ebner *et al.* (1987), Wrobel (1987), Barnard (1987), and Shibasaki and Murai (1986). As shown in Rauhala *et al.* (1988), the main advantage of GLSC is its high quality which improves the overall production timeline by orders of magnitude. The increase in reliability of two-ray correlation from 50 to 80 percent to the order of 99 percent would reduce

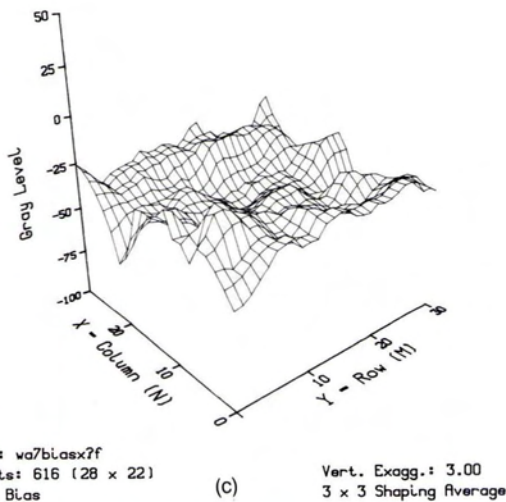
Island



Island



Wall



Wall

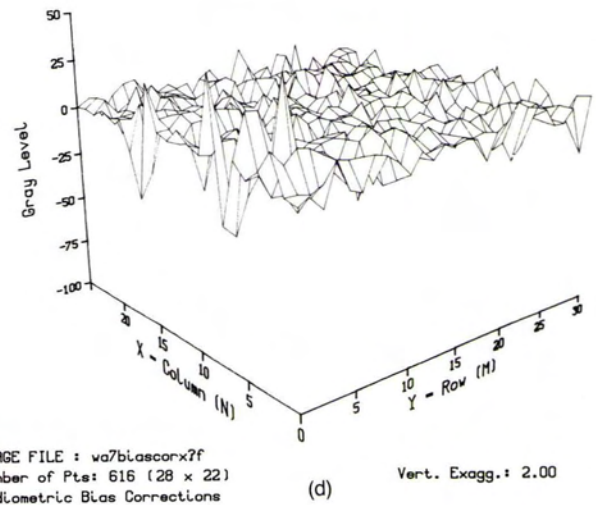


FIG. 5. (a) 3x3 shaping average of radiometric bias of optimal Is solution. (b) Correction terms of radiometric bias of optimal Is solution. (c) 3x3 shaping average of radiometric bias of optimal Wall solution. (d) Correction terms of radiometric bias of optimal Wall solution.

the manual bottleneck by a factor of 50 to 20.\* The implementation of the multi-ray and multi-layer GLSC of Rauhala (1986) will further improve the quality, speed, and economy of CPS, making digital photogrammetry competitive with conventional mapping systems. This will also apply to automated large-scale mapping over urban, forestry, and mountainous areas.

ACKNOWLEDGMENTS

Jas Arnold and Vince Kluth prepared the figures and edited the text of this paper. The main coding work of the GLSC algorithm was done during 1986-88 by Ken Baker, Don Davis, and Jas Arnold. Dr. Uki Helava shared the ISPRS data tape of the Stuttgart ISPRS working group III/4.

REFERENCES

Barnard, S. T., 1987. *Stereo Matching by Hierarchical Microcanonical Annealing*. Technical Note No. 414, SRI International, Menlo Park, California.

Bergstrom, J., 1974. *An Investigation of Gingival Topography in Man by Means of Analytical Photogrammetry*. Doctoral Thesis, Karolinska Institute, Stockholm.

Blahe, G., 1987. *Nonlinear Parametric Least-Squares Adjustment*. Scientific Report No. 1, Air Force Geophysics Laboratory, Hanscom AFB, Massachusetts 01731

Brown, D. C., 1984. A Large Format, Microprocessor Controlled Film Camera Optimized for Industrial Photogrammetry. Paper presented at ISPRS Congress, Comm V, Rio de Janeiro.

Cooley, J., and J. Tukey, 1965. An Algorithm for Machine Computation of Complex Fourier Series. *Math Comput.* Vol. 19.

Ebner, H., D. Fritsch, W. Gillessen, and C. Heipke, 1987. Integration von Bildzuordnung und Objektrekonstruktion innerhalb der Digitalen Photogrammetrie. *Bul 5*.

Good, I. J., 1958. The Interaction Algorithm and Practical Fourier Series. *J. Royal Stat. Soc., Ser. B*, 20.

\*The 10 to 20 times increase of accuracy from 1-2 pe of the conventional DTM correlation to the order of 0.1 pe would allow 10 to 20 times smaller image scale and 100 to 400 times larger area coverage, making the combined speeding factor to 2,000 to 20,000. Multiply this by 100 to 1,000 for a parallel processor implementation of GLSC.

- Gruen, A., and E. Baltsavias, 1986. High Precision Image Matching for Digital Terrain Model Generation. *ISPRS Comm III Proceedings*, Rovaniemi.
- , 1987. Geometrically Constrained Multiphoto Matching. *ISPRS Intercommission Conference on Fast Processing of Photogrammetric Data*, Interlaken.
- Helava, U. V., 1987. The Digital Comparator Correlator System (DCCS). *ISPRS Intercommission Conference*, Interlaken.
- Lippert, F. G., 1973. The Feasibility of Photogrammetry as a Clinical Research Tool. *J. Biomechanics* 6.
- Lugnani, J. B., and F. C. B. Souza, 1984. Control Features - An Alternative Source for Urban Area Control. *ISPRS Congress, Comm III*, Rio de Janeiro.
- Masry, S. E., 1981. Digital Mapping Using Entities: A New Concept *Photogrammetric Engineering and Remote Sensing*, No. 11.
- Rauhala, U. A., 1968. *Geodeettisten ja fotogrammetristen havaintojen yhteistason soveltamismahdollisuuksista erikoisesti rajojen ja runkopisteiden mittaukseen*. Dipl. eng. thesis, Helsinki Univ. of Technology.
- , 1972. Calculus of Matrix Arrays and General Polynomial and Harmonic Interpolation by Least Squares with New Solutions in Photogrammetry and Geodesy. *Fot. Medd. VI: 4*, Dept. of Photogrammetry, Royal Institute of Technology, Stockholm.
- , 1974. Array Algebra with Applications in Photogrammetry and Geodesy. *Fot. Medd. VI: 6*, Stockholm.
- , 1975. Calculation of Loop Inverses. *ASP Spring Convention*, March, Washington, D.C.
- , 1976. A Review of Array Algebra. *Comm III, ISPRS Congress*, Helsinki and *Fot. Medd. 2:38*, Stockholm.
- , 1977. Array Algebra as General Base of Fast Transforms. *Comm. III, Image Processing Symposium ISP*, Graz.
- , 1978. Array Algebra DTM. *DTM Symposium*, 9–11 May, St. Louis, ASP
- , 1980a. *Development of Array Algebra Algorithms for Finite Element Filtering*. Final Report, DMA Contract 700-78-C-0022P00002, Geodetic Services Inc.
- , 1980b. Introduction to Array Algebra. *Photogrammetric Engineering and Remote Sensing*, No. 2.
- , 1980c. Experiments Using Array Algebra DTM Algorithms. *ASP Convention*, St. Louis.
- , 1980d. Experimental Array Algebra Modeling Algorithms. *Comm. III ISPRS Congress*, Hamburg.
- , 1981. Note on General Linear Estimators and Matrix Inverses. *Manuscript Geodaetica*, Vol 6.
- , 1982. Array Algebra Estimation in Signal Processing. *Photogrammetric Engineering and Remote Sensing*, No. 9.
- , 1984. Array Algebra Approach of Self-Calibrating Inertial Traverse and Net Adjustments. *ACSM Spring Meeting*, Washington, D.C.
- , 1986. Compiler Positioning of Array Algebra Technology. *Int. Arch. of ISPRS*, Vol. 26-3/3, *Comm. III Symposium*, Rovaniemi.
- , 1987. Fast Compiler Positioning Algorithms and Techniques of Array Algebra in Analytical and Digital Photogrammetry. *Proceedings of Intercommission ISPRS Conference on Fast Processing of Photogrammetric Data*, Interlaken, 2–4 June.
- Rauhala, U. A., and S. Gerig, 1976. *Digital Terrain Data Compression Using Array Algebra*. USA-ETL report DAAG53-76-C-0127.
- Rauhala, U. A., D. Davis, and K. Baker, 1988. Automated DTM Validation and Progressive Sampling Algorithm of Finite Element Array Relaxation. *ASPRS Spring Convention*, St. Louis.
- Rosenholm, D., 1986. Accuracy Improvement of Digital Matching for Evaluation of Digital Terrain Models. *ISPRS Comm. III Symposium*, Rovaniemi.
- Rosenholm, D., and K. Torlegard, 1987. Absolute Orientation of Stereo Models Using Digital Elevation Models. *ASPRS Convention Proceedings*, Baltimore.
- Shibasaki, R., and S. Murai, 1986. Stereo Matching for Stereo Mode CCD Linear Sensors. *ISPRS Comm. III Symposium*, Rovaniemi.
- Siegwarth, J. D., J. F. LaBrecque, and C. L. Carroll, 1984. Volume Uncertainty of a Large Tank Calibrated by Photogrammetry. *Photogrammetric Engineering and Remote Sensing*, No. 8.
- Wrobel, B., 1987. Facets Stereo Vision-A New Approach to Computer Vision and to Digital Photogrammetry. *ISPRS Intercommission Conference*, Interlaken.

(Received 25 May 1988; accepted 21 July 1988)

### Forthcoming Articles

- Steven G. Ackleson and Patrick M. Holligan, AVHRR Observations of a Gulf of Maine Coccolithophore Bloom.
- Lee De Cola, Fractal Analysis of a Classified Landsat Scene.
- Mohamed Shawki Elghazali, Analytical Independent Model Triangulation Strip Adjustment Using Shore-Line Constraints.
- Sabry F. El-Hakim, A Hierarchical Approach to Stereo Vision.
- J.H. Everitt, D.E. Escobar, M.A. Alaniz, and M.R. Davis, Using Multispectral Video Imagery for Detecting Soil Surface Conditions.
- Nancy A. Felix and Daryl L. Binney, Accuracy Assessment of a Landsat-Assisted Vegetation Map of the Coastal Plain of the Arctic National Wildlife Refuge.
- John G. Fryer and Scott O. Mason, Rapid Lens Calibration of a Video Camera.
- Armin W. Gruen, Digital Photogrammetric Processing Systems — Current Status and Prospects.
- Susumu Hattori, Shunji Murai, Hitoshi Ohtani, and Ryosuke Shibasaki, A Semi-Automatic Terrain Measurement System for Earthwork Control.
- Michael E. Hodgson and Reese W. Plews, N-Dimensional Display of Cluster Means in Feature Space.
- Urho A. Rauhala, Don Davis, and Ken Baker, Automated DTM Validation and Progressive Sampling Algorithm of Finite Element Array Relaxation.
- Donald C. Rundquist, Richard O. Hoffman, Marvin P. Carlson, and Allen E. Cook, The Nebraska Center-Pivot Inventory: An Example of Operational Satellite Remote Sensing on a Long-Term Basis.
- J. Sneddon and T.A. Lutze, Close-Range Photogrammetric Measurement of Erosion in Coarse-Grained Soils.
- N.H. Thyer, J.A.R. Blais, and M.A. Chapman, High Altitude Laser Ranging Over Rugged Terrain.
- Qiming Zhou, A Method for Integrating Remote Sensing and Geographic Information Systems.